Architectural Design, Interior Decoration, and Three-Dimensional Plumbing en Route to Multifunctional Nanoarchitectures

JEFFREY W. LONG AND DEBRA R. ROLISON*

Surface Chemistry Branch, Code 6170, Naval Research Laboratory, Washington, D.C. 20375

Received December 18, 2006

ABSTRACT

Ultraporous aperiodic solids, such as aerogels and ambigels, are sol–gel-derived equivalents of architectures. The walls are defined by the nanoscopic, covalently bonded solid network of the gel. The vast open, interconnected space characteristic of a building is represented by the three-dimensionally continuous nanoscopic pore network. We discuss how an architectural construct serves as a powerful metaphor that guides the chemist in the design of aerogel-like nanoarchitectures and in their physical and chemical transformation into multifunctional objects that yield high performance for rate-critical applications.

Introduction

Quantum dots; nanorods, nanotubes, and their multipodal relatives; nanoparticles evoking shapes reminiscent of Platonic perfect solids; dendritic clusters that burst into tree or star shapes: A well-stocked inventory of morphologies on the nanoscale exists and encompasses the compositional richness of chemistry, all in a journal near you. In one view—in our view—these nanoscopic bits of matter are mere unit quantities that can be assembled into multifunctional (and far more interesting) objects: nanoarchitectures.

Just as nano is not new to chemists, neither are nanoarchitectures. And just as architects design buildings[1] that can follow a rigid rectilinear hierarchy or may eschew orthogonality for the functional whimsy of Calatrava (Figure 1) or Gehry, so, too, can chemists design well-ordered nanoarchitectures (suitable for applications demanding high periodicity, e.g., photonics) or aperiodic edifices of immediate technological relevance (e.g., the thermal superinsulation used on Martian rovers).

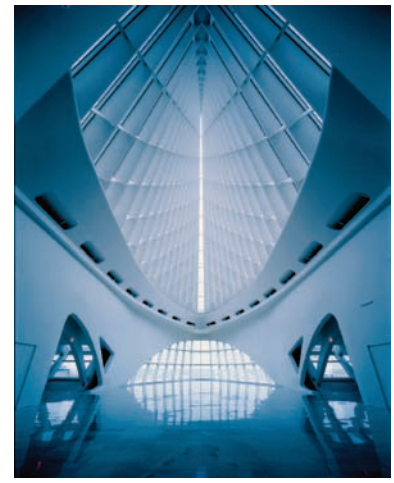

FIGURE 1. Architectural function (and flair) achieved without regularity or periodicity dominating form. The Milwaukee Art Museum, Windhover Hall; architect, Santiago Calatrava; photo, Timothy Hursley (with permission of the Milwaukee Art Museum).

The sol–gel-derived aperiodic nanoarchitectures known as aerogels date to Kistler's recognition in the 1930s that removing pore fluid without establishing a liquid–vapor interface yields an air-filled solid that retains the free volume of the wet gel.[2] In that the liquid has an open, three-dimensionally interconnected path throughout the wet gel, so does air through an aerogel. A related nanoarchitecture known as an ambigel,[3] also exhibiting open, through-connected porosity, is obtained when a low-surface tension, nonpolar fluid is evaporated from a wet gel under ambient pressure rather than the supercritical pressures used to obtain aerogels.

Aerogels and ambigels are composites of being and nothing.[4] These nanoarchitectures have a physical structure that contains 75–99% open space (the "nothing") interpenetrated by solid matter (the "being"). Unlike other open cellular foams, these materials are "all nano, all the time", with the solid sized on the order of 10 nm and the pores predominantly sized from 10 to 100 nm (i.e., mesoporous to macroporous).[5] A further advantage of these ultraporous nanoarchitectures is that they are innately self-wired: the nanoscopic solids, diluted within a sea of nothing, are covalently networked and thereby constrained in their mobility and ability to agglomerate or sinter into larger particles. As befits nanomaterials in use since the 1930s, aerogels underpin scientific studies and cutting-edge technology from Čerenkov radiation detectors to thermal superinsulation (e.g., in clothing for extreme sports) to collecting cosmic dust in space (NASA's Stardust mission).

The architectural metaphor on the nanoscale offers a powerful analogy for chemistry. Buildings are mostly nothing for a functional reason: the interconnected open spaces are critical for the movement of people and objects into, out of, and within the structure. The interpenetrating, open pore network characteristic of aerogel-like architec-

Jeffrey Long received a B.S. in Chemistry with Honors from Wake Forest University (Winston-Salem, NC) in 1992. Working with Professor Royce Murray, he earned a Ph.D. in Chemistry from the University of North Carolina (Chapel Hill, NC) in 1997. His research focuses on nanostructured materials, particularly hybrid nanoarchitectures for applications in sensing, separations, and electrochemical energy storage and conversion. E-mail: jeffrey.long@nrl.navy.mil.

Debra Rolison received a B.S. in Chemistry from Florida Atlantic University (Boca Raton, FL) in 1975 and a Ph.D. in Chemistry from the University of North Carolina in 1980 under the direction of Royce W. Murray. She joined the Naval Research Laboratory as a research chemist in 1980 and currently heads the Advanced Electrochemical Materials section; she is also an Adjunct Professor of Chemistry at the University of Utah (Salt Lake City, UT). Her research at the NRL focuses on multifunctional nanoarchitectures with special emphasis on catalysis, energy storage and conversion, biomolecular composites, porous magnets, and sensors. E-mail: rolison@nrl.navy.mil.

 10.1021/ar6000445
Published on Web 05/26/2007

tures likewise permits rapid transport of molecules and nanoscopic objects into, throughout, and out of the structure. With this ability to import raw materials into the nanoarchitecture, the chemist/architect can then serve as an interior designer, physicochemically modifying the surfaces of the inner walls (painting, laying carpet) or decorating with objets d'art.

A temptation when adding functionality into porous solids is to use the void space as a molecular beaker whereby the nothing often becomes filled. This nanoscopic nothing is too important to fill up, especially as it must be maintained through-connected to achieve high performance in rate-critical applications (e.g., catalysis, sensing, energy storage and conversion, and separations) such that one maximizes the number of molecules reacted per second or electrons transferred per second.[6] An electrician would never electrically wire a building by templating conductive wires that filled rooms or corridors, nor would a designer paint the walls with foot-thick coatings. If the nanotechnologist in her role as architect/interior designer/electrician/plumber takes similar care when chemically altering the confined, tortuous interior of nanoarchitectures such as aerogels, she will be rewarded with multifunctional materials that significantly impact a broad range of end uses, as we detail below.

Building the Structural Frame: Synthesis of Three-Dimensional (3D) Multifunctional Walls

Sol–gel chemistry erects the walls of the nanoarchitecture as a concomitant outcome of the sol-to-gel transition. The nanoscopic solid network takes shape as the colloidal particles dispersed in the sol covalently bond together; once formed, the network delineates space and does so within the dimensions of the vessel in which gelation occurs. Nanoarchitectures can thus be particulates, films, and monolithic shapes of all types that reflect the container into which the sol was poured. In the absence of a templating shape for formation of periodic mesoporous solids,[7] sol–gel chemistry is a protocol that fabricates aperiodic, self-connected walls. But the solid network in an aerogel or ambigel can be so much more than merely a framework that defines the shape and volume of the building.

Establishing Form with Function that Goes Beyond Delineating Space. Constructing the solid network—the walls of the structure—from materials that contribute specific physical and chemical properties imparts functionality to the resulting edifice. For example, nanoarchitectures fabricated from electrically conductive building blocks have been explored for a wide range of electrochemical applications.[3,8] Carbon aerogels, prepared by pyrolyzing a phenolic polymer aerogel, have served as ultraporous, high-surface area electrode structures for electrochemical capacitors[9,10] and capacitive deionization.[11] Carbon aerogels once decorated with electrocatalytic metals transform into porous structures suitable for fuel-cell reactions.[12–14]

Erecting walls of mixed ion–electron conducting metal oxides with compositions such as V_2O_5[15–17] and MnO_2[18–21] provides energy-storage functionality via cation–electron insertion, while the high-quality plumbing and wiring of the nanoarchitecture enable high-rate charge–discharge operation. When the solid network comprises oxygen-ion conducting oxides, such as ceria, zirconia, and doped variants, the nanoarchitectural form provides optimally accessible gas–solid interfaces for oxygen dissociation and ionic conduction,[22–24] elementary processes that are critical for the operation of solid–oxide fuel cells. Semiconducting TiO_2 aerogels functionalized with ruthenium polypyridyl photosensitizing dyes enhance absorption of long-wavelength visible photons,[25] which is the underperforming region of the solar spectrum for mesoporous titania photoanodes in dye-sensitized solar cells.

Importance of Self-Constructed Walls. A key property of electrically conductive aerogel-type nanoarchitectures is the innate interconnectivity of the solid nanoscopic skeleton, which provides for efficient long-range and redundant electrical wiring throughout the structure. Good wiring not only is critical for the electrochemical performance of these structures for applications such as batteries, fuel cells, and electrochemical capacitors but also enables the use of electrodeposition methods to further "decorate" the nanoarchitecture in a self-limiting manner (see below).[26–28] Conductive-probe atomic force microscopy, which yields simultaneous topography and current images, was recently used to test the electrical character of MnO_2 ambigel films supported on indium–tin oxide glass.[29] The relative uniformity of the current image (Figure 2b) and its correlation with the topography image (Figure 2a) indicate that electrical conductivity through the 1.5-μm thick, ultraporous 3D structure of the MnO_2 nanoarchitecture is largely homogeneous.

The long-range continuity of the architecture is also vital for efficient ionic conduction, as demonstrated by impedance studies for monolithic MnO_2 ambigels exposed to controlled levels of humidity at room temperature.[30] We ascribed the Warburg, diffusion-like feature in the resulting impedance spectra to the formation of a "proton wire", present even at 11% relative humidity. The nanoscopic oxide network templates a conformal and confined sheath of adsorbed water layers that traverse the macroscopic dimensions of the MnO_2 ambigel monolith. The proton wire thus established exhibits macroscopically long proton diffusion lengths (>0.3 mm) and an equilibrium conductometric response to humidity that is 14 times greater than that of previous reports for films of electrolytic manganese oxide.[30] An analogous ion wire, also with long-range diffusion lengths, was observed for an entirely different conduction process, the conduction of oxygen ions at 600 °C in gadolinium-doped ceria aerogels.[24]

Other Physical Properties of Walls: Photoactivity, Magnetism. As useful as electrically conductive nanoarchitectures are, recent work imparts new directions in multifunctional nanoarchitectures by extending the functionality of the framework to magnetic materials and photoactive semiconductors. Kinetically controlled oxida-

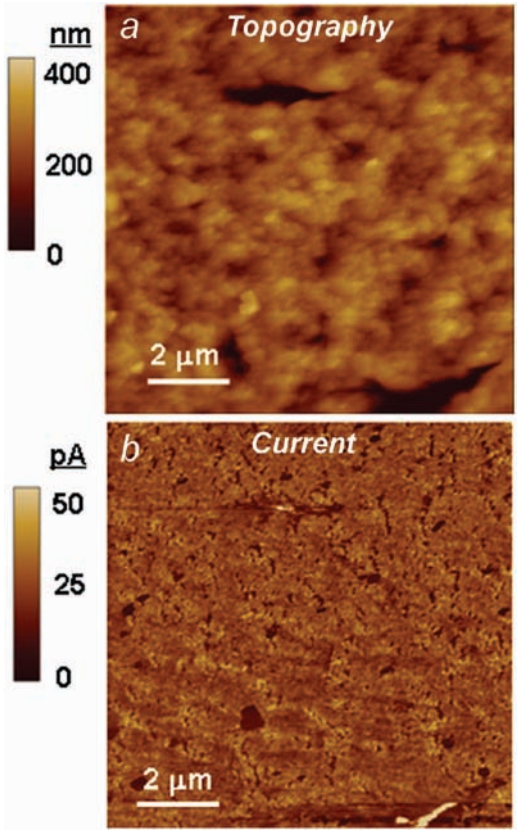

FIGURE 2. Simultaneously acquired (a) topography and (b) current images (10 μm $\times$ 10 μm) of a birnessite-type MnO_2 ambigel film supported on indium–tin oxide coated glass. Reproduced from ref 29. Copyright 2006 American Chemical Society.

tion of the capping ligands from sols of CdSe, CdS, ZnS, and PbS quantum dots induces gel formation and, upon supercritical drying, photoluminescent aerogels that span the infrared through ultraviolet regions of the electromagnetic spectrum.[31,32] The mesoporous, covalently interconnected nanoarchitectures retain the quantum-confined optical properties characteristic of the semiconducting nanoparticles used to build the gel.

Superparamagnetic nanoarchitectures have been prepared by appropriate temperature–atmosphere treatments of amorphous iron oxide aerogels.[33] Once crystallized, the nanoarchitectures can be reversibly tuned between either Fe_3O_4 (magnetite) or γ-Fe_2O_3 (maghemite) phases by varying the partial pressure of O_2 at mild temperatures, ~250 °C (see the Supporting Information for a movie demonstrating the ability of a Fe_3O_4 aerogel to counter gravity upon magnetization at room temperature). Coupling microprobe Raman spectroscopy (which gauges the local structure and cation vacancy content) with magnetic analysis readily differentiates between these structurally similar nanocrystalline oxides, unlike the ambiguity in assignment via X-ray or electron diffraction. The synthetic strategy used to construct magnetic iron oxide nanoarchitectures has been extended to the family of transition metal ferrites, as seen for $MnFe_2O_4$ aerogels.[34]

Earthquake-Proofing the Structure. Low-density aerogel/ambigel materials are often mechanically fragile as a consequence of the many weak points that exist where the individual building blocks of the nanoarchitecture are bonded together, the so-called particle–particle necks. Strategies for improving the ruggedness of aerogels, which will improve their commercial prospects, typically focus on reinforcing and widening these neck regions. For example, Leventis and co-workers have used organic cross-linking agents that react with surface hydroxyl or amine functionalities to produce polymeric tethers that further reinforce the framework of silica aerogels, resulting in materials that are 2 orders of magnitude stronger than unmodified aerogels.[35,36]

Strengthening the structure is crucial not only for the end uses of the nanoarchitecture but also to facilitate some of the additional interior design that is needed to create multifunctional nanoarchitectures. Any modification strategy that requires re-wetting the architecture is made feasible when the pore–solid nanoarchitecture can withstand the compressive forces of wetting and dewetting. Certain postconstruction modifications may be hindered, however, by the presence of organic reinforcements. We have shown that the ruggedness of silica aerogels can be enhanced by rapid gelation, immediate immersion in neat methanol (i.e., curing in the absence of mother liquor), and then calcining the supercritically dried gel at 900 °C for 30 min (which modestly densifies the nanoarchitecture).[37] Cured aerogels lose less volume at 900 °C relative to gels processed in the standard way (i.e., aged in the mother liquor) and retain larger average pore sizes (30 nm vs 16 nm). The interparticle necks are deduced to be less fragile in the cured gels, presumably because the flux of oligomers out of the gel upon immersion in neat methanol forces condensation reactions to occur at the most reactive internal points, i.e., the interparticle necks and the mouths of micropores and small mesopores. The cured, 900 °C-calcined aerogels are 80% nothing, can be dropped without breaking, and immersed in or removed from water without damage.

3D Plumbing and the Importance of Nothing

The nature of the porous network in sol–gel-derived materials is readily transformed by how pore fluid is removed from the wet gel; see Figure 3a. The exact nature of the pore-size distribution depends on the composition and mechanical characteristics of the solid network, but the trends are similar between the oxide gels. Xerogels are obtained by drying under conditions of high surface tension (often from the aqueous/alcoholic mother liquor) and thereby suffer extensive pore collapse. A xerogel retains 20 to <50% of the initial free volume inherent to the wet gel with a pore-size distribution dominated by micropores (<2 nm) and small mesopores. The pore-size distributions for ambigels and aerogels shift to larger pore sizes, with the aerogel distribution dominated by macropores (>50 nm) and large mesopores.[21] The ambigel has a Gaussian-like distribution of pores, with few of the micropores or small mesopores typical of xerogels and far fewer of the large mesopores or macropores typical of

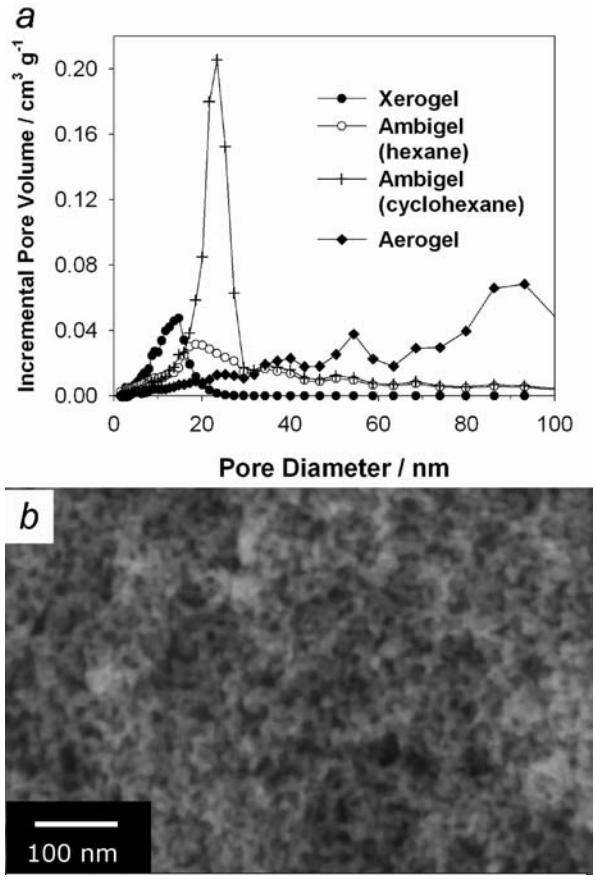

FIGURE 3. (a) Plots of pore-size distribution for various nanoarchitectures of sol–gel-derived birnessite $Na_\delta MnO_2 \cdot xH_2O$ (cylindrical pore model). Reproduced from ref 21. Copyright 2001 American Chemical Society. (b) Scanning electron micrograph of a birnessite ambigel revealing the mesoporous nature of the 3D plumbing.

aerogels (Figure 3a,b). The pore size at the maximum of the relatively narrow pore-size distribution seen for ambigels can be shifted by varying the temperature at which the nonpolar organic pore fluid is evaporated.[38]

Aperiodic, Through-Connected 3D Porosity = Open-Medium Diffusion Rates. Gas-adsorption isotherms indicate an open, connected porosity for xerogels or templated periodic solids with 3D mesoporosity, as do the isotherms obtained for aerogel and ambigel nanoarchitectures. It is only with rate-critical, not equilibrium, measurements that the quality of the porous network can be assessed,[3,6] such as permeation through membranes and influx of reactants into sensing or catalytic architectures or the electrically conductive structures necessary for energy storage or conversion. A critical aspect of the internal structure of aerogel-like solids is the retention of that structure within objects of any size, from films that are 100-nm thick to particulate chunks of aerogel to monoliths that are blocks 1 m^2. Periodic mesoporous solids can lose the registry of their porosity at length scales over a few micrometers.

In aerogels and ambigels, the rate at which a gas-phase solute diffuses through the pore–solid architecture approaches its rate of diffusion in open air,[39] which means that an aerogel-based device has what every rate-critical application needs, a veritable autobahn for molecular

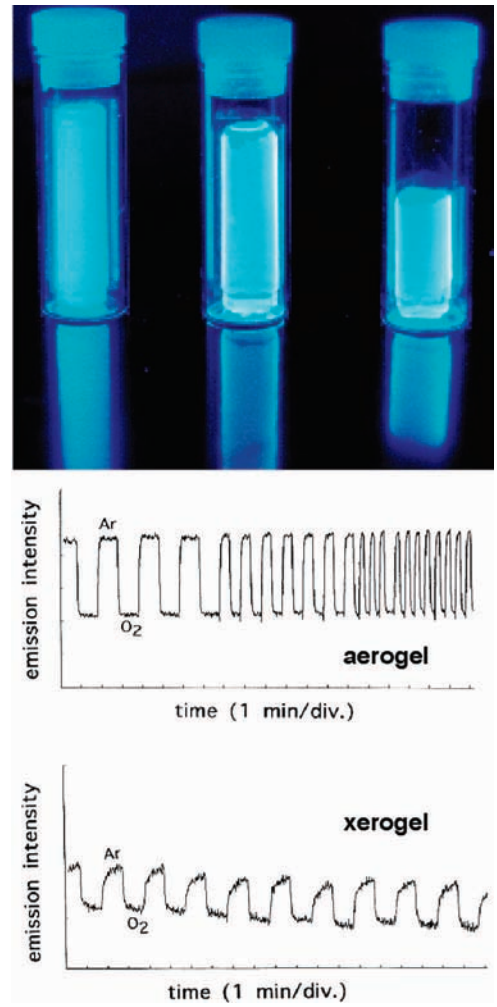

FIGURE 4. Diazapyrenium-modified silica aerogel (1-cm thick) responds nearly instantaneously to O_2 as compared to a 1.4-mm thick diazapyrenium-modified silica xerogel. In the photograph, the leftmost gel is bulk modified with the fluorophore via copolymerization, while the two aerogels on the right are modified only at the boundary of the monolith. This selectivity permits small-molecule analytes to be distinguished from entities (e.g., viruses and cells) too bulky to enter the pore network. Reproduced from ref 39. Copyright 1999 American Chemical Society.

transport. Figure 4 shows the rapid steady-state response attained by a fluorophore-modified silica aerogel upon switching between gas-phase analytes that either quench (oxygen) or restore (argon) the native fluorescence of the diazapyrenium modifier. Processing the wet, fluorophore-modified gel to form a xerogel markedly slows the time response to analyte and affects the return to background (full fluorescence under Ar). When one needs to know—now—that a deadly gas-phase species is present, the choice between sensing architectures is obvious.

This dramatic contrast in the time signature of the fluorophore-modified aerogel versus its xerogel cousin arises because aerogels retain not only an open porosity but also a 3D through-connected pore structure, i.e., one without the cave-ins that are inevitable in xerogels because of the compressive forces that arise internally during the drying process. In our comparisons of the time response of a chemically diverse range of xero/ambi/aerogels under

flux conditions, aerogel and ambigel nanoarchitectures consistently respond 10–100 times faster than do xerogels. For instance, self-organized cytochrome *c* superstructures encapsulated in 5-mm thick silica aerogels exhibit more rapid recognition of NO(g) than 5-μm thick silica xerogel films containing encapsulated cytochrome *c*.[40] In many respects, designing sensors using a xerogel platform is a waste of time.

The essentially unrestricted diffusive transport characteristic of ambigels and aerogels allows molecular access to the high specific surface area of the solid network, which amplifies the reaction zone; in silica aerogels, the surface:volume ratio is 10^6. This architectural feature also improves reactivity under forcing conditions. Manganese oxide aerogels insert Li ions without fading over four cycles under high-rate conditions (1 A discharge/0.5 A charge), while at these rates, the xerogel form loses the ability to communicate with 60% of the active material after the first discharge.[41] The importance of the through-connectedness of the void volume can also be demonstrated by comparing the electrical response times at 600 °C to changes in atmosphere (between O_2 and Ar) for agglomerated nanocrystalline ceria of comparable surface area, crystallite size, and void volume to ceria aerogel and ambigel nanoarchitectures: the nanoarchitectures respond 4 times faster.[23]

Interior Decoration

Once a carefully designed nanoarchitecture is realized, with electromagnetically interactive wiring and high-quality plumbing in place, the functionality of the edifice can be further enhanced through interior decoration. In the process of decorating, however, one must be careful not to obstruct the continuity of the pore network (the 3D plumbing) as new components are brought into the nanoarchitecture from the outside world.

Bringing in Paint, Carpet, and Objets d'Art. Achieving control of the decorating process is particularly challenging when modifying macroscopically thick nanoarchitectures because the inhomogeneous supply and flux of molecular, ionic, or nanoscopic precursors from the outside world (the contacting precursor phase) favor deposition at the boundary of the nanoarchitecture (see Scheme 1). To overcome hermetically sealing the nanoarchitecture when applying a coating, one must use deposition processes that are inherently self-limiting. In this approach, the coating is initiated at the surface of the walls of the nanoarchitecture, which are then passivated toward further reaction by the coating. Thus, even though the deposition may initially be favored at the boundary of the structure, the rapid passivation of the surface ensures that the coating does not become thick enough to clog the pipes and hinder further transport of precursors to the interior of the nanoarchitecture for further reaction.

Self-limiting electropolymerization schemes have been used to paint electrically conductive manganese oxide[26,28] and carbon[27] nanoarchitectures with ultrathin (<15-nm thick), conformal polymers. This concept was recently extended to electroless deposition processes, specifically the redox reaction of aqueous permanganate with the walls of carbon nanofoam substrates, resulting in the formation of self-limiting, nanoscopic deposits of electroactive manganese(III/IV) oxide that permeate the entire structure.[42] This simple modification retains the open pore network and provides 1.5 F of capacitance per square centimeter of device geometric footprint with minimal optimization of the state of the nanoscopic oxide or the pore network of the carbon nanofoam; standard MnO_2-based capacitors provide <100 mF/cm^2.

Scheme 1. Cross-Sectional Illustration of Poorly Controlled versus Self-Limiting Deposition onto Aperiodic Nanoarchitectures from Solution-Phase Precursors

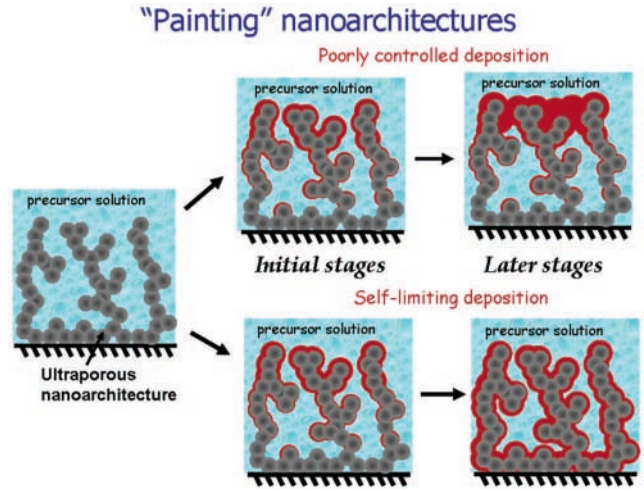

Atomic-layer deposition (ALD) also offers a self-limiting deposition process but is distinguished from the electrochemical and electroless deposition processes described above by the use of many alternating self-limiting layers of oxides or metals, as applied to a substrate via gas-phase reactants. The use of ALD has recently been extended to aerogels in producing coatings of ZnO on silica[43] and tungsten/tungsten oxide on carbon.[44]

Another way to thwart runaway deposition at the exterior of the nanoarchitecture is by equilibrating throughout the interior a precursor with a low sticking coefficient and a triggered reactivity, e.g., by temperature or photoactivation. We developed a cryogenic route to conformally pave 1% of the solid network in silica aerogel with 2-nm spheres of nanoscopic, anhydrous RuO_2 that deposited in a self-connected path upon thermal decomposition of adsorbed RuO_4 at approximately −35 °C. Upon being heated in oxygen to ~150 °C, the nanoparticles crystallized into 2-nm high, 4-nm wide, and 10–40-nm long laths of rutile RuO_2, thereby converting an electrically silent architecture (insulating silica aerogel) into a self-wired, water- and air-stable nanoscopic metallic conductor.[45] Variations on chemical vapor deposition using ruthenocene and $Ru(CO)_{12}$ precursors reliably produced isolated, pore-filling globules of nanoscopic RuO_2 at the processing temperatures necessary to convert the Ru precursor into either metal or oxide,[46] whereas the

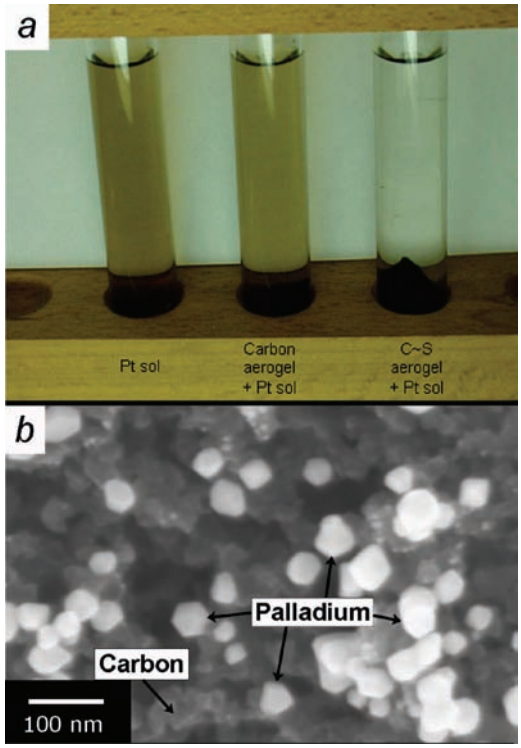

FIGURE 5. (a) Photograph of aliquots of Pt (~2-nm) sol before (left) and after mixing with unmodified carbon aerogel (center) and thiophenylated carbon aerogel (right). Reproduced from ref 13. Copyright 2004 Elsevier. (b) Scanning electron micrograph of thiophenylated carbon aerogel exposed to aqueous Pd sol.

cryogenic route yields the desired web of nanowires conformally riding the surface of the silica network.[45]

Hanging Discrete Objects on the Wall. In some cases, it may be desirable to use preformed objects, such as colloidal metal nanoparticles, as an active component of a multifunctional nanoarchitecture. By designing the walls of the nanoarchitecture with chemically specific "hooks" that capture such objects as they are introduced into the structure, one can simultaneously achieve good particle dispersion and strong adhesion to the substrate.

We followed this strategy with phenolic polymer aerogels by covalently modifying the polymeric gel with a low weight percentage of thiophene. The sulfur moiety survives pyrolysis to form an electronically conductive carbon aerogel with thiophene-like surface functionalities.[13] The thiophenyl moiety replicates the anchor site that makes Vulcan carbon such a successful support.[47] When introduced into carbon aerogels, the sulfur hook spontaneously adsorbs metal nanoparticles from aqueous sols flowing into the structure (see Figure 5).

The resulting metal-modified structure maximizes the exposure of the nanoparticle surface to the void space of the nanoarchitecture (see Figure 5b), which is a critical aim in any application where the nanoparticle serves as a catalytic element, for example, fuel cells. Counting the number of Pt surface atoms for Pt-modified, thiophenylated carbon aerogels by adsorbing carbon monoxide and then electrochemically stripping the adsorbate demonstrated that up to 86% of the expected Pt surface atoms are accessible.[13]

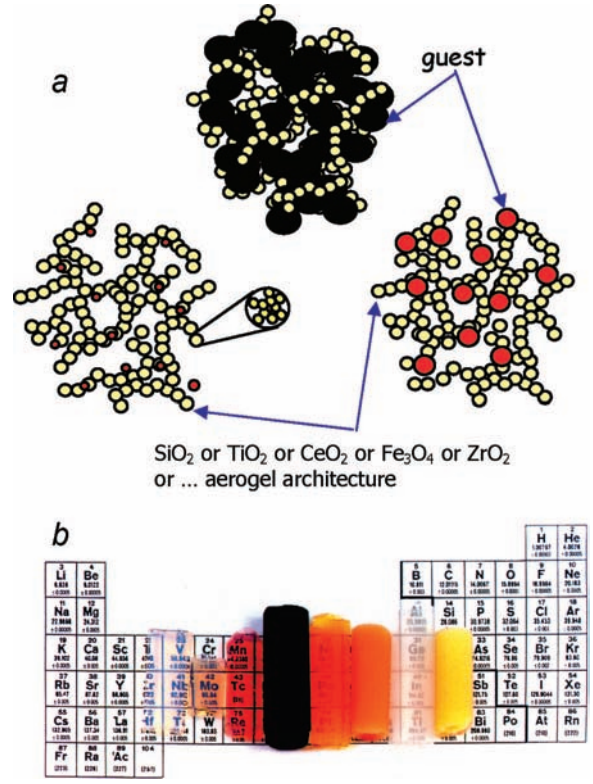

FIGURE 6. (a) Schematic of guest–host composite aerogels for guests that are comparable in size to, smaller than, and larger than the colloidal oxide sol that nanoglues the guest into the solid network upon gelation. (b) Photograph of silica-based composite aerogels (from left to right): silica aerogel (overlaying Groups 4 and 5 in the periodic table), Pt–silica (2-nm Pt), Au–silica (30-nm Au), carbon black–silica (Vulcan carbon XC-72), poly(methylmethacrylate)–silica (polymer $M_w \sim 15000$, sieved to $<44\ \mu$m), $Fe^{II}(bpy)_3$NaY zeolite–silica (0.1–1-μm type Y zeolite crystallites modified with Fe^{II}tris-bipyridine), titania–silica (micrometer-sized pieces of TiO_2 aerogel), and titania–silica (~40-nm TiO_2 Degussa P-25). All samples shown are ~1 cm diameter monoliths. Reproduced from ref 50. Copyright 2000 Wiley.

Interior Decoration While Assembling the Structural Frame: Nanogluing. Although the surface hydroxyls on oxide aerogels are molecular points onto which to graft a wealth of organic and organometallic functionality, and even oxide colloids,[48] we have also demonstrated a simple means of incorporating new functionality without the need to have a reactive linker on the desired guest. We do so via nanogluing (Figure 6): a process whereby guest particles added to an about-to-gel sol are incorporated into the nanoscale oxide framework upon the sol-to-gel transition.[49–51] The network-forming reactions remain driven by the oxide sol, not the guest particles. The oxide nanoglue may be derived from among the wealth of oxide sols known in the literature, and the guests can range over 6 orders of magnitude in size from nanometers to millimeters.

Adding the guest shortly before gelation allows it to escape complete encapsulation by colloidal oxide particles such that some fraction of the surface area of the guest remains available to react with molecular solutes traveling though the pore network.[49,51] The number density of guest

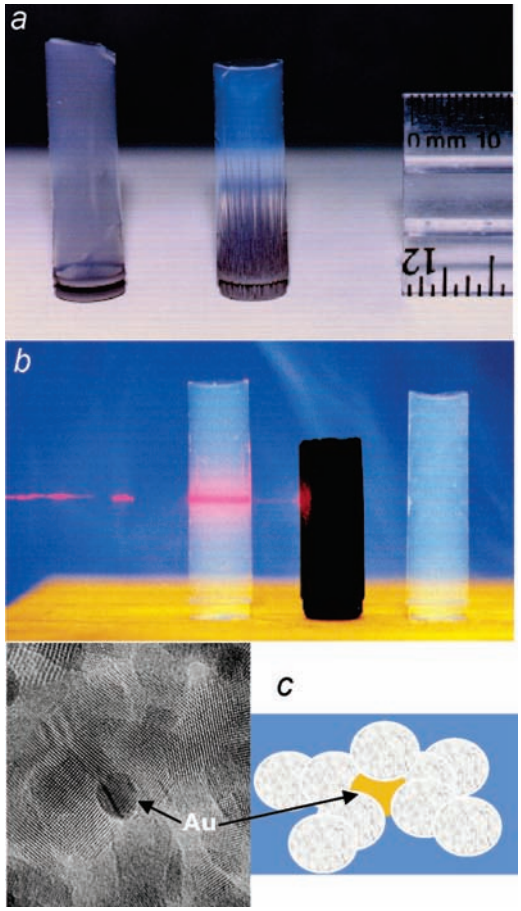

FIGURE 7. (a) Photograph of Fe–silica composite aerogels containing 15-μm Fe particles that were added to an about-to-gel silica sol with (right) and without (left) an applied 4.6-T magnetic field. Reproduced from ref 53. Copyright 2002 American Chemical Society. (b) Photograph of a He–Ne laser (from left) irradiating air, a silica aerogel, and a Vulcan carbon–silica composite aerogel. No light transmits through the carbon–silica composite aerogel to irradiate the rightmost silica aerogel. Reproduced from ref 50. Copyright 2000 Wiley. (c) Micrographic (left) and schematic (right) depiction of the enhancement in Au–TiO_2 contacts within catalytic Au–TiO_2 composite aerogels; 6-nm Au particle nestled amidst comparably sized anatase TiO_2. Reproduced from ref 54. Copyright 2002 American Chemical Society.

particles in the nanoarchitecture can be varied above and below a percolation threshold for electrical or thermal transport paths between guest particles (Figure 6a), depending on the properties desired for the end use. Self-associating guests (e.g., carbon blacks and carbon nanotubes) can achieve transport networks within a composite gel/aerogel at levels lower than percolation thresholds.[49,52] Note that because aerogels are fractal materials, with a fractal dimension of <3, slightly higher number densities are required to reach percolating networks relative to a 3D composite. For example, the electrical properties of a mixed oxide aerogel of RuO_2 and TiO_2 were TiO_2-dominated at a composition of $(RuO_2)_{0.2}$-$(TiO_2)_{0.8}$ but RuO_2-dominated at $(RuO_2)_{0.32}$-$(TiO_2)_{0.68}$.[4]

By providing a simple means of shifting the functionality of the guest–host nanoarchitecture, nanogluing is every interior designer's dream tool kit. Functional variants can

Scheme 2. Schematic Showing the Three Steps Needed to Assemble a Fully Interpenetrating Nanoscale Battery in Which All Three Functional Components (cathode–ion-conducting separator–anode) Are Sized on the Order of 10 nm and Are Separated by <50 nm

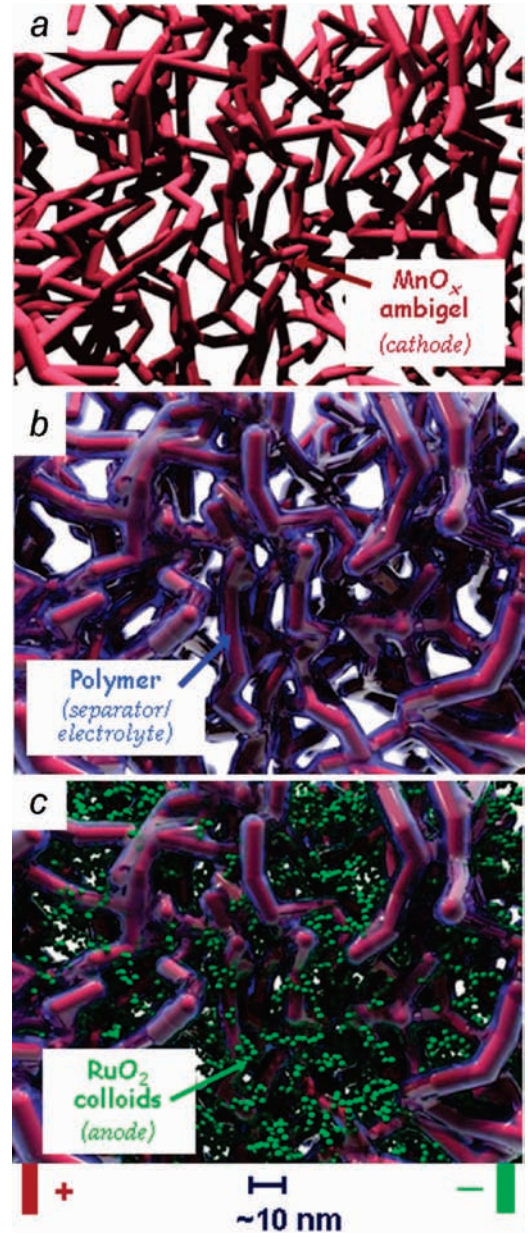

range from gradient-aligned porous materials created by using magnetic guests and applying a magnetic field during the sol-to-gel transition (Figure 7a)[53] to turning a transparent, 85% open architecture into a trap for visible light by adding carbon black (Figure 7b)[49,50] to inverting the flea-on-the-boulder form of traditional bifunctional catalysts (where the support is at least 10 times larger than the catalytic nanoscopic metal) into a cooperative structure in which each catalytic nanoparticle is physically linked to multiple, comparably sized crystallites of the oxide network (Figure 7c).[54] The only restriction to the functional versatility of the resultant nanoarchitecture is the cleverness of the designer.

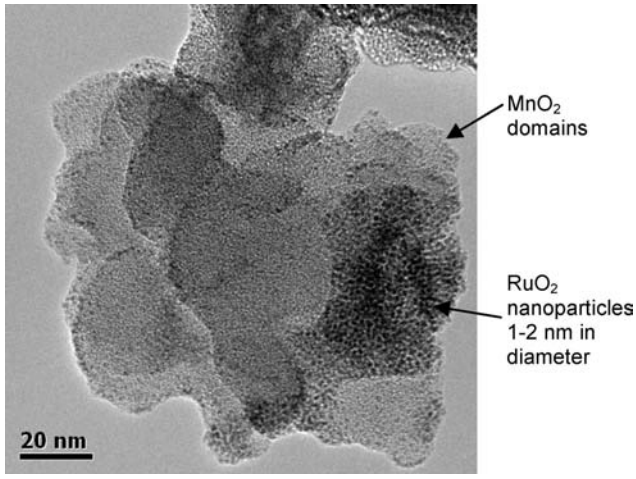

FIGURE 8. Transmission electron micrograph of MnO_2–poly(phenylene oxide) after deposition of nanoscopic RuO_2 via the cryogenic decomposition of RuO_4. Reproduced from ref 56. Copyright 2006 American Chemical Society.

21st-Century Multifunctional Nanoarchitectures

To illustrate how applying the full architectural metaphor to aerogels can affect the way we look at very old technology, consider the sequential steps shown in Scheme 2 in which a cation-insertion framework (e.g., manganese dioxide[20]) is painted by a pinhole-free, ultrathin polymer separator [e.g., poly(phenylene oxide)[28]], leaving sufficient free volume to introduce a second cation-insertion phase (e.g., nanoscopic RuO_2[55]). The MnO_2–polymer–RuO_2 nanoarchitecture that results becomes a solid-state nanoscopic battery, fully integrated in three dimensions.

Transmission electron microscopic characterization of such a tricontinuous composite shows that RuO_2, cryogenically deposited within the nanoarchitecture, remains nanoscopic and self-aggregates (i.e., wires) its way throughout the nanoarchitecture (Figure 8).[56] The microscopy also provides important information about the nature of the MnO_2–poly(phenylene oxide) interface: although birnessite MnO_2 domains can still be viewed by TEM, their characteristic lattice fringes are not, thereby indicating that the polymer film electrodeposits within the MnOx nanoarchitecture and does so as an ultrathin layer.

Aerogels have presented nanoarchitectural opportunities since the 1930s and have been technologically relevant, sol–gel-derived materials for decades. The advent of new compositions for the networked frame and new ways to decorate the interior of these high surface-to-volume materials expand even further the potential of these pore–solid nanoarchitectures for 21st century nanoscience and technology.

We acknowledge the U.S. Office of Naval Research and the U.S. Defense Applied Research Projects Agency for support of our program on multifunctional nanoarchitectures. We especially thank our undergraduate and postdoctoral research associates and faculty visitors for accompanying us on this architectural adventure on the nanoscale.

Supporting Information Available: Movie demonstrating the ability of a Fe_3O_4 aerogel to counter gravity upon magnetization. This material is available free of charge via the Internet at http://pubs.acs.org.

References

(1) *Architecture Week* http://www.greatbuildings.com/architects.html.
(2) Kistler, S. S. Coherent expanded aerogels and jellies. *Nature* **1931**, *127*, 741.
(3) Rolison, D. R.; Dunn, B. Electrically conductive oxide aerogels: New materials in electrochemistry. *J. Mater. Chem.* **2001**, *11*, 963–980.
(4) Swider, K. E.; Merzbacher, C. I.; Hagans, P. L.; Rolison, D. R. Synthesis of RuO_2-TiO_2 aerogels: Redistribution of electrical properties on the nanoscale. *Chem. Mater.* **1997**, *9*, 1248–1255.
(5) Hüsing, N.; Schubert, U. Aerogels airy materials: Chemistry, structure, and properties. *Angew. Chem., Int. Ed.* **1998**, *37*, 23–45.
(6) Rolison, D. R. Catalytic nanoarchitectures—The importance of nothing and the unimportance of periodicity. *Science* **2003**, *299*, 1698–1701.
(7) Sanchez, C.; Julian, B.; Belleville, P.; Popall, M. Applications of hybrid organic-inorganic nanocomposites. *J. Mater. Chem.* **2005**, *15*, 3559–3592.
(8) Owens, B. B.; Passerini, S.; Smyrl, W. H. Lithium ion insertion in porous metal oxides. *Electrochim. Acta* **1999**, *45*, 215–224.
(9) Fischer, U.; Saliger, R.; Bock, V.; Petricevic, R.; Fricke, J. Carbon aerogels as electrode material in supercapacitors. *J. Porous Mater.* **1997**, *4*, 281–285.
(10) Pekala, R. W.; Farmer, J. C.; Alviso, C. T.; Tran, T. D.; Mayer, S. T.; Miller, J. M.; Dunn, B. Carbon aerogels for electrochemical applications. *J. Non-Cryst. Solids* **1998**, *225*, 74–80.
(11) Farmer, J. C.; Fix, D. V.; Mack, G. V.; Pekala, R. W.; Poco, J. F. Capacitive deionization of NaCl and $NaNO_3$ solutions with carbon aerogel electrodes. *J. Electrochem. Soc.* **1996**, *143*, 159–169.
(12) Glora, M.; Wiener, M.; Petričević, R.; Pröbstle, H.; Fricke, J. Integration of carbon aerogels in PEM fuel cells. *J. Non-Cryst. Solids* **2001**, *285*, 283–287.
(13) Baker, W. S.; Long, J. W.; Stroud, R. M.; Rolison, D. R. Sulfur-functionalized carbon aerogels: A new approach for loading high-surface-area electrode nanoarchitectures with precious metal catalysts. *J. Non-Cryst. Solids* **2004**, *350*, 80–87.
(14) Marie, J.; Berthon-Fabry, S.; Achard, P.; Chatenet, M.; Pradourat, A.; Chainet, E. Highly dispersed platinum on carbon aerogels as supported catalysts for PEM fuel cell-electrodes: Comparison of two different synthesis paths. *J. Non-Cryst. Solids* **2004**, *350*, 88–96.
(15) Le, D. B.; Passerini, S.; Tipton, A. L.; Owens, B. B.; Smyrl, W. H. Aerogels and xerogels of V_2O_5 as intercalation hosts. *J. Electrochem. Soc.* **1995**, *142*, L102–L103.
(16) Salloux, K.; Chaput, F.; Wong, H. P.; Dunn, B.; Breiter, M. W. Lithium intercalation in vanadium pentoxide aerogels. *J. Electrochem. Soc.* **1995**, *142*, L191–L192.
(17) Dong, W.; Dunn, B.; Rolison, D. R. Electrochemical properties of high surface area vanadium oxide aerogels. *Electrochem. Solid-State Lett.* **2000**, *3*, 457–459.
(18) Passerini, S.; Coustier, F.; Giorgetti, M.; Smyrl, W. H. Li-Mn-O aerogels. *Electrochem. Solid-State Lett.* **1999**, *2*, 483–485.
(19) Long, J. W.; Swider-Lyons, K. E.; Stroud, R. M.; Rolison, D. R. Design of pore and matter architectures in manganese oxide charge-storage materials. *Electrochem. Solid-State Lett.* **2000**, *3*, 453–456.
(20) Long, J. W.; Stroud, R. M.; Rolison, D. R. Controlling the pore–solid architecture of mesoporous, high-surface-area manganese oxides with the birnessite structure. *J. Non-Cryst. Solids* **2001**, *285*, 288–294.
(21) Long, J. W.; Qadir, L. R.; Stroud, R. M.; Rolison, D. R. Spectroelectrochemical investigations of cation-insertion reactions in sol–gel-derived nanostructured, mesoporous thin films of manganese oxide. *J. Phys. Chem. B* **2001**, *105*, 8712–8717.
(22) Chervin, C. N.; Clapsaddle, B. J.; Chiu, H. W.; Gash, A. E.; Satcher, J. H.; Kauzlarich, S. M. Aerogel synthesis of yttria-stabilized zirconia by a non-alkoxide sol-gel route. *Chem. Mater.* **2005**, *17*, 3345–3351.
(23) Laberty-Robert, C.; Long, J. W.; Lucas, E. M.; Pettigrew, K. A.; Stroud, R. M.; Doescher, M. S.; Rolison, D. R. Sol–gel-derived ceria nanoarchitectures: Synthesis, characterization and electrical properties. *Chem. Mater.* **2006**, *18*, 50–58.
(24) Laberty-Robert, C.; Long, J. W.; Pettigrew, K. A.; Stroud, R. M.; Rolison, D. R. Ionic nanowires at 600 °C: Using nanoarchitecture to optimize electrical transport in nanocrystalline gadolinium-doped ceria. *Adv. Mater.* **2007**, *19*, in press.
(25) Pietron, J. J.; Stux, A. M.; Compton, R. S.; Rolison, D. R. Dye-sensitized titania aerogels as photovoltaic electrodes for electrochemical solar cells. *Sol. Energy Mater. Sol. Cells* **2007**, *91*, 1066–1074.

(26) Long, J. W.; Rhodes, C. P.; Young, A. L.; Rolison, D. R. Ultrathin, protective coatings of poly(*o*-phenylenediamine) as electrochemical proton gates: Making mesoporous MnO_2 nanoarchitectures stable in acid electrolyte. *Nano Lett.* **2003**, *3*, 1155–1161.
(27) Long, J. W.; Dening, B. M.; McEvoy, T. M.; Rolison, D. R. Carbon aerogels with ultrathin electroactive poly(*o*-methoxyaniline) coatings for high-performance electrochemical capacitors. *J. Non-Cryst. Solids* **2004**, *350*, 97–106.
(28) Rhodes, C. P.; Long, J. W.; Doescher, M. S.; Dening, B. M.; Rolison, D. R. Charge insertion into hybrid nanoarchitectures: Mesoporous manganese oxide coated with ultrathin poly(phenylene oxide). *J. Non-Cryst. Solids* **2004**, *350*, 73–79.
(29) McEvoy, T. M.; Long, J. W.; Smith, T. J.; Stevenson, K. J. Nanoscale conductivity mapping of hybrid nanoarchitectures: Ultrathin poly(*o*-phenylenediamine) on mesoporous manganese oxide ambigels. *Langmuir* **2006**, *22*, 4462–4466.
(30) Doescher, M. S.; Pietron, J. J.; Dening, B. M.; Long, J. W.; Rhodes, C. P.; Edmondson, C. A.; Rolison, D. R. Using oxide nanoarchitectures to make or break a proton wire. *Anal. Chem.* **2005**, *77*, 7924–7932.
(31) Mohanan, J. L.; Arachchige, I. U.; Brock, S. L. Porous semiconductor chalcogenide aerogels. *Science* **2005**, *307*, 397–400.
(32) Arachchige, I. U.; Brock, S. L. Sol-gel assembly of CdSe nanoparticles to form porous aerogel networks. *J. Am. Chem. Soc.* **2006**, *128*, 7964–7971.
(33) Long, J. W.; Logan, M. S.; Rhodes, C. P.; Carpenter, E. E.; Stroud, R. M.; Rolison, D. R. Magnetic pore–solid nanoarchitectures of magnetite (Fe_3O_4) and maghemite (γ-Fe_2O_3): Synthesis, characterization, and magnetic properties. *J. Am. Chem. Soc.* **2004**, *126*, 16879–16889.
(34) Long, J. W.; Logan, M. S.; Carpenter, E. E.; Stroud, R. M.; Rolison, D. R. Synthesis and characterization of Mn-FeOx aerogels with magnetic properties. *J. Non-Cryst. Solids* **2004**, *350*, 182–188.
(35) Leventis, N.; Sotoriou-Leventis, C.; Zhang, G. H.; Rawashdeh, A. M. M. Nanoengineering strong silica aerogels. *Nano Lett.* **2002**, *2*, 957–960.
(36) Meador, M. A. B.; Fabrizio, E. F.; Ilhan, F.; Dass, A.; Zhang, G. H.; Vassilaras, P.; Johnston, J. C.; Leventis, N. Cross-linking amine-modified silica aerogels with epoxies: Mechanically strong lightweight porous materials. *Chem. Mater.* **2005**, *17*, 1085–1098.
(37) Lucas, E. M.; Doescher, M. S.; Wahl, K. J.; Ebenstein, D. M.; Rolison, D. R. Silica aerogels with enhanced mechanical strength, 30-nm mean pore diameter, and improved immersibility in water. *J. Non-Cryst. Solids* **2004**, *350*, 244–252.
(38) Barrow, A. J.; Lytle, J. C.; Long, J. W.; Rolison, D. R. Unpublished results, Naval Research Laboratory, 2006.
(39) Leventis, N.; Elder, I. A.; Anderson, M. L.; Rolison, D. R.; Merzbacher, C. I. Durable modification of silica aerogel monoliths with fluorescent 2,7-diazapyrenium moieties. Sensing oxygen near the speed of open-air diffusion. *Chem. Mater.* **1999**, *11*, 2837–2845.
(40) Wallace, J. M.; Rice, J. K.; Pietron, J. J.; Stroud, R. M.; Long, J. W.; Rolison, D. R. Silica nanoarchitectures incorporating self-organized protein superstructures with gas-phase bioactivity. *Nano Lett.* **2003**, *3*, 1463–1467.
(41) Long, J. W.; Stroud, R. M.; Rolison, D. R. Controlling the pore–solid architecture of mesoporous, high-surface-area manganese oxides with the birnessite structure. *J. Non-Cryst. Solids* **2001**, *285*, 288–294.
(42) Fischer, A. E.; Pettigrew, K. A.; Stroud, R. M.; Rolison, D. R.; Long, J. W. Incorporation of homogeneous, nanoscale MnO_2 within ultraporous carbon structures via self-limiting electroless deposition: Implications for electrochemical capacitors. *Nano Lett.* **2007**, *7*, 281–286.
(43) Kuncheyev, S. O.; Biener, J.; Wang, Y. M.; Baumann, T. F.; Wu, K. J.; van Buuren, T.; Hamza, A. V.; Satcher, J. H.; Elam, J. W.; Pellin, M. J. Atomic layer deposition of ZnO on ultralow-density nanoporous silica aerogel monoliths. *Appl. Phys. Lett.* **2005**, *86*, 083108.
(44) Elam, J. W.; Libera, J. A.; Pellin, M. J.; Zinovev, A. V.; Greene, J. P.; Nolen, J. A. Atomic layer deposition of W on nanoporous carbon aerogels. *Appl. Phys. Lett.* **2006**, *89*, 053124.
(45) Ryan, J. V.; Berry, A. D.; Anderson, M. L.; Long, J. W.; Stroud, R. M.; Cepak, V. M.; Browning, V. M.; Merzbacher, C. I.; Rolison, D. R. Electronic connection to the interior of a mesoporous insulator with nanowires of crystalline RuO_2. *Nature* **2000**, *406*, 169–172.
(46) Merzbacher, C. I.; Barker, J. G.; Long, J. W.; Rolison, D. R. The morphology of nanoscale deposits of ruthenium oxide in silica aerogels. *Nanostruct. Mater.* **1999**, *12*, 551–554.
(47) Swider, K. E.; Rolison, D. R. The chemical state of sulfur in carbon-supported fuel cell electrodes. *J. Electrochem. Soc.* **1996**, *143*, 813–819.
(48) Morris, C. A.; Rolison, D. R.; Swider-Lyons, K. E.; Osburn-Atkinson, E. J.; Merzbacher, C. I. Modifying nanoscale silica with itself: A method to control surface properties independently of bulk structure. *J. Non-Cryst. Solids* **2001**, *285*, 29–36.
(49) Morris, C. A.; Anderson, M. L.; Stroud, R. M.; Merzbacher, C. I.; Rolison, D. R. Silica sol as a nanoglue: Flexible synthesis of composite aerogels. *Science* **1999**, *284*, 622–624.
(50) Anderson, M. L.; Stroud, R. M.; Morris, C. A.; Merzbacher, C. I.; Rolison, D. R. Tailoring advanced nanoscale materials through synthesis of composite aerogel architectures. *Adv. Eng. Mater.* **2000**, *2*, 481–488.
(51) Anderson, M. L.; Morris, C. A.; Stroud, R. M.; Merzbacher, C. I.; Rolison, D. R. Colloidal gold aerogels: Preparation, properties, and characterization. *Langmuir* **1999**, *15*, 674–681.
(52) Sakamoto, J. S.; Dunn, B. Vanadium oxide-carbon nanotube composite electrodes for use in secondary lithium batteries. *J. Electrochem. Soc.* **2002**, *149*, A26–A30.
(53) Leventis, N.; Elder, I. A.; Long, G. J.; Rolison, D. R. Using nanoscopic hosts, magnetic guests, and field alignment to create anisotropic composite gels and aerogels. *Nano Lett.* **2002**, *2*, 63–67.
(54) Pietron, J. J.; Stroud, R. M.; Rolison, D. R. Using three dimensions in nanostructured mesoporous catalysts. *Nano Lett.* **2002**, *2*, 545–549.
(55) Lytle, J. C.; Rhodes, C. P.; Long, J. W.; Pettigrew, K. A.; Stroud, R. M.; Rolison, D. R. The importance of combining disorder with order for Li-ion insertion into cryogenically prepared nanoscopic ruthenia. *J. Mater. Chem.* **2007**, *17*, 1292–1299.
(56) Long, J. W.; Rhodes, C. P.; Lytle, J. C.; Pettigrew, K. A.; Stroud, R. M.; Rolison, D. R. Integrating the multifunction necessary for 3-D batteries into mesoporous nanoarchitectures. *Polym. Prepr. Papers (Am. Chem. Soc., Div. Fuel Chem.* **2006**, *51*, 41–43.

AR6000445